Separation Science and Technology
Publication details, including instructions for authors and subscription information:
http://www.informaworld.com/smpp/title~content=t713708471

HIGH-GRADIENT MAGNETIC SEPARATION FOR THE TREATMENT OF HIGH-LEVEL RADIOACTIVE WASTES

Armin D. Ebner[a]; James A. Ritter[a]; Luis Nuñez[b]
[a] Department of Chemical Engineering, Swearingen Engineering Center, University of South Carolina, Columbia, SC [b] Chemical Technology Division, Argonne National Laboratory, Argonne, IL

To cite this Article Ebner, Armin D. , Ritter, James A. and Nuñez, Luis(1999) 'HIGH-GRADIENT MAGNETIC SEPARATION FOR THE TREATMENT OF HIGH-LEVEL RADIOACTIVE WASTES', Separation Science and Technology, 34: 6, 1333 — 1350
To link to this Article: DOI: 10.1080/01496399908951096
URL: http://dx.doi.org/10.1080/01496399908951096

SEPARATION SCIENCE AND TECHNOLOGY, 34(6&7), pp. 1333–1350, 1999

HIGH-GRADIENT MAGNETIC SEPARATION FOR THE TREATMENT OF HIGH-LEVEL RADIOACTIVE WASTES

Armin D. Ebner and James A. Ritter*
Department of Chemical Engineering
Swearingen Engineering Center
University of South Carolina,
Columbia, SC 29208

Luis Nuñez
Chemical Technology Division
Argonne National Laboratory
Argonne, IL 60439

ABSTRACT

Argonne National Laboratory is developing an open-gradient magnetic separation (OGMS) system to fractionate and remove nonglass-forming species from high-level radioactive wastes (HLW); however, to avoid clogging, OGMS may require high-gradient magnetic separation (HGMS) as a pretreatment to remove the most magnetic species from the HLW. In this study, the feasibility of using HGMS in the pretreatment of HLW was demonstrated. A HLW simulant of Hanford's C-103 tank waste, which contained precipitated hydroxides and oxides of Fe, Al, Si, and Ca, was used. Preliminary fractionation results from a 0.3-T bench-scale HGMS unit showed that a significant amount of Fe could be removed from the HLW simulant. Between 1 and 2% of the total Fe in the sludge was removed during each stage, with over 18.5% removed in the 13 stages that were carried out. Also, in each stage, the magnetically retained fraction contained about 20% more Fe than the untreated HLW; however, it also contained a significant amount of SiO_2 in relatively large particles. This indicated that SiO_2 was acting possibly as a nucleation agent for Fe (i.e, an Fe adsorbent) and that the fractionation was based more on size than on magnetic susceptibility.

*Author for correspondence. E-mail: ritter@sun.che.sc.edu.

INTRODUCTION

High-gradient magnetic separation (HGMS) is a process that has been designed especially for removing magnetic particles that cannot be separated with other traditional magnetic separation processes because of their lower paramagnetic properties and smaller size (1). The HGMS process basically consists of a fine ferromagnetic wire matrix (e.g., stainless steel wool) inserted in the bore of a magnet, which is then energized by an externally applied magnetic field. The external magnetic field creates large magnetic field gradients around the fine ferromagnetic wires, thereby improving the removal efficiency of relatively small and only weakly magnetic particles.

HGMS has been used extensively in the early 1970's by the kaolin clay industry to remove iron and other magnetic impurities (1–3). Also, HGMS has proven applications in mineral benefication, waste reclamation and recycling, and ultrapurification of chemical refractories and powders (4–15). Other applications of HGMS, some still under development, include environmental remediation and nuclear waste treatment (16–20), and contaminated water treatment with magnetite, which is used either as a metal-ion adsorbent or as a magnetic seeding agent for nonmagnetic particles (21–28). Additional, rather novel applications of HGMS include biomagnetic separations, where enzymes, viruses, and cells are removed by coating them with magnetic oxides (29–31), or they are fractionated by coating magnetic particles with bio-selective materials (32).

Recently, with the decision for using vitrification as the final waste form in the United States for the long-term storage of high-level radioactive waste (HLW) (33), there is renewed interest in using magnetic field processes for removing spinel-forming compounds from HLW, since these compounds may have a profound effect on the quality and stability of the final glass product. The presence or formation of ferrites or spinels during the vitrification process may create separated crystalline phases within the amorphous structure of the glass, resulting in a brittle and less durable product (34). An HGMS system may be capable of removing some of the iron and other spinel-forming species in the HLW, but not the most weakly magnetic species. However, an open-gradient magnetic separation (OGMS) system (35–38), placed downstream of an HGMS system, may be capable of removing the weakly magnetic species.

OGMS has been investigated at the Oak Ridge (35), Los Alamos (36) and Argonne National Laboratories (37,38) for fractionating weakly paramagnetic materials from

plutonium fly ash wastes, coal, and cracking catalysts containing small amounts of nickel. In all of these studies, the waste streams consisted of dry powders. Very recently, however, OGMS is being investigated for the fractionation of HLW (39), which is a new application of OGMS, since HLW streams consist of wet slurries.

The objective of this paper is to demonstrate the feasibility of the HGMS process for the treatment of HLW. The idea is to first use HGMS to remove the most magnetic fraction of the HLW, which is composed mainly of Fe, Ni, Co, Cr, Ti, Mn, and some lanthanides (which may cause clogging in an OGMS unit), and then to use OGMS for fractionating any remaining weakly paramagnetic and smaller particles. Initial work has been carried out with a HLW simulant of Hanford's C-103 tank waste. Preliminary fractionation results from a 0.3-T bench-scale HGMS unit have been obtained and are discussed below.

EXPERIMENTAL

Preparation of C-103 Simulant

The C-103 Hanford tank waste simulant was prepared by the Pacific Northwest National Laboratory (PNNL) according to the following procedure: 24.5 kg of $Fe(NO_3)_3 \cdot 9H_2O$ was added to 73 L of deionized (DI) water and stirred until dissolved. A sufficient quantity of 5 *M* NaOH (about 36.5 L) was added to obtain a pH of 7.5. The solution was stirred for 30 min, and 13.0 kg of 50 wt % colloidal SiO_2 (0.1 μm, Nyacol silicasol 9950) was added and stirred. Then 1.4 kg of gibbsite (0.25 μm, Alcoa SpaceRite S-11), 0.4 kg boehmite (20 nm, Vista Catapal) and 2.6 kg of $Ca_{10}(OH)_2(PO_4)_6$ were added to the solution. Next, 5 *M* NaOH was added slowly while stirring until pH 12 was reached; vigorous stirring was continued for 24 h. Finally, 5 *M* HNO_3 was added slowly while stirring until pH 10 was reached, and then sufficient DI water was added to give a final volume of 200 L. The final simulant was stirred for an additional 3 h.

HGMS System and Experimental Procedure

An HGMS system from Advanced Environmental Systems, Inc., was used in this study; a schematic is shown in Figure 1. This 0.3-T HGMS system (A) has a magnetic

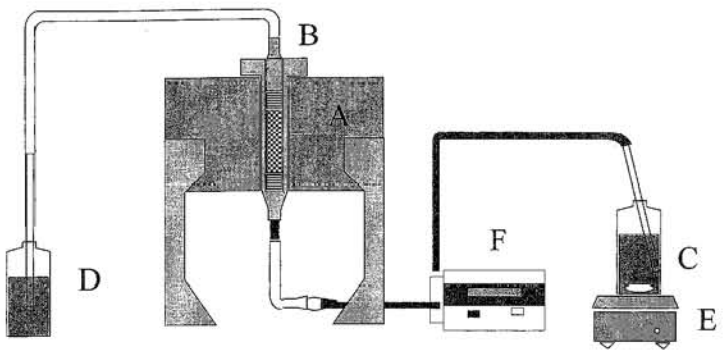

FIGURE 1. Schematic of the 0.3-T HGMS unit: (A) 0.3-T magnet; (B) filter canister; (C) feed solution; (D) effluent solution; (E) magnetic stirrer; (F) peristaltic pump.

bore that is 4.75 in. long and 2.06 in. in diameter, with a filter canister (B) area of 0.01 ft^2 (i.e., 4.75 in. long and 1.375 in. in diameter). The filter canister includes magnetic pole pieces that serve to evenly distribute the magnetic field over the matrix area. The matrix consists of graded expanded metal and about 30 g of steel wool discs stacked within the canister to a maximum height of 4.75 in. The element size of the steel wool discs varies between 200 and 500 μm. This HGMS system has been field tested by the manufacturer, where they claim at least 99% of the iron, cobalt, magnetite, and other spinels and ferrites, at least 50% of the hematite, and at least 30% of the hydrated irons (FeO*OH species), all of particle sizes greater than 0.1 μm, can be removed from aqueous streams.

In the tests carried out in this study, the C-103 simulant (C) was passed upward through the canister to ensure complete flooding; and the effluent was collected in a 1-L bottle (D). The feed solution was continuously stirred with a magnetic stirrer (E) and transported at a flow rate of 150 mL/min with a peristaltic pump (F) placed just before the separation unit. The experimental procedure is depicted in Figure 2. Initially, the magnetic field was turned on and 1 L of the C-103 simulant was passed through the magnet. All of the effluent was collected and denoted as the head. Then, with the magnet still turned on, pH 10 distilled water was passed upward through the magnet to remove the loosely attached and least magnetic particles from the stainless steel matrix

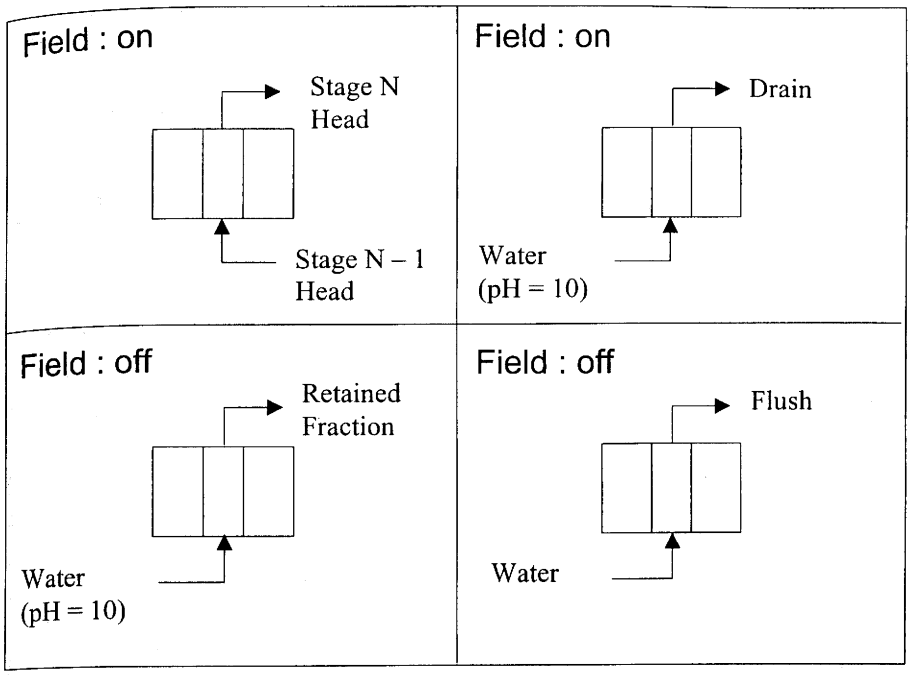

FIGURE 2. Depiction of the four-step experimental procedure.

and to confirm the presence of a magnetically retained fraction within the stainless steel mesh. This effluent solution, denoted as the drain, was collected until it became noticeably dilute. Then, while still continuously passing pH 10 distilled water, the magnetic field was turned off to remove and collect the magnetically retained fraction. This deeply colored effluent was collected until it became noticeably dilute. Finally, with the field turned off, the magnet was flushed with distilled water to prepare it for the start of a new stage. This new stage was initiated by passing the head solution collected from the previous stage through the HGMS system, and so went the cycle from stage to stage. Thirteen stages were processed this way. All of these fractions were stirred and sampled for subsequent analysis, including a sample from the C-103 simulant that was denoted as initial.

Procedure Used for Sample Analysis

Three different analyses were carried out on the three separate fractions from each stage and on an initial sample. Initially, three aliquots were taken from each of the fractions of the first four stages to determine the volumetric particle size distributions (VPSDs) and mean particle sizes, in triplicate, using a Nicomp^{TM} 370 Submicron Particle Sizer. Then all of the samples (i.e., the initial sample and all of the fractions from each of the 13 stages) were completely vacuum filtered using Gelman Sciences 0.45-μm Tuffryn® membrane filters and dried overnight under vacuum (-0.6 atm) and at room temperature to maintain the particle size distribution. The dried initial sample and the samples from first stage were analyzed in a Hitachi 2500Δ Scanning Electron Microscope (SEM) integrated with a Kevex Quantum Elemental Dispersive X-ray Analyzer (EDAX). SEM micrographs and elemental weight percentages of the samples were obtained. Finally 0.5 g of each sample was digested for 2 h at 100 °C in 6 mL of nitric acid (50 wt %) in sealed 30-mL Teflon tubes. The resulting liquid and solid phases were denoted as digestible and nondigestible phases, respectively. The phases were separated using vacuum filtration and Gelman Sciences 0.45-μm Tuffryn® membrane filters and then the liquid phase was adequately diluted prior to analyzing its metal content (Fe, Al, Ca, and Si) using a Perkin Elmer 3300 Flame Atomic Absorption (AA) Spectrometer. The nondigestible phase was a very fine white powder as opposed to the typical brownish color of the sludge; it was assumed to be SiO_2.

RESULTS AND DISCUSSION

Characterization of C-103 Simulant

Table 1 lists the physical characteristics of the C-103 simulant. Table 2 compares the results of the metal analyses obtained with the flame AA with those calculated from the sludge recipe. Table 3 presents the results obtained with EDAX in terms of the relative weight percentages of the predominant metals in the initial sludge.

Very small amounts of Fe, Al, Ca, and Si were detected in the soluble phase, which implied that almost all of these metals were in solid or nonsoluble states. After

TABLE 1. BULK METAL CONTENT AND PHYSICAL PROPERTIES OF THE C-103 HANFORD SLUDGE SIMULANT

pH	8.80
Total solids, wt %	17.05
Insoluble solids, wt %	9.20
Soluble solids, wt %	7.13
Density, g/mL	1.08
Digestible Fraction of Insoluble Phase (mg/g)[a]	
Fe	212.73
Al	37.35
Ca	40.00
Si	ND[b]
Nondigestible Fraction of insoluble Phase (mg/g)[a]	
SiO_2 and CaO	327.00
Soluble Phase (mg/L)[c]	
Fe	< 0.40
Al	< 0.20
Ca	3.20
Si	ND[b]

[a] Based on insoluble solids.
[b] Not detected.
[c] Based on total sludge volume.

TABLE 2. COMPARISON OF THE BULK METAL CONTENT OF THE SLUDGE OBTAINED WITH FLAME AA WITH THAT CALCULATED FROM THE PNNL RECIPE

Element	Flame AA (mg/L)[a]				Recipe (mg/L)
	Soluble	Digested	Nondigested	Total	
Fe	<0.4	18,121	-	18,121	16,950
Al	<0.2	3,183	-	3,183	3,450
Ca	3.92	3,407	-	3,411	5,200
Si	-	-	27,856	27,856	32,550

[a] Based on total sludge volume.

TABLE 3. RELATIVE ELEMENTAL WEIGHT PERCENTAGES AND RATIOS FROM ELEMENTAL DISPERSIVE X-RAY ANALYSES OF THE INSOLUBLE SOLIDS IN THE INITIAL SAMPLE AND DIFFERENT FRACTIONS FROM THE FIRST STAGE

	wt %			
Element	Initial	Head	Drain	Retained
Fe	49.7	47.3	40.7	61.8
Si	30.6	34.3	38.2	25.2
Ca	11.0	10.7	12.7	5.6
Al	4.8	5.3	6.2	3.6
Cu	3.6	2.3	2.0	3.6

	wt % ratio			
Ratio	Initial	Head	Drain	Retained
Fe/Al	10.3	9.0	6.6	17.1
Si/Al	6.3	6.5	6.2	6.9
Ca/Al	2.3	2.0	2.0	1.6

filtering and treating the nonsoluble phase with nitric acid, Fe, Al, and Ca were detected in the digestible phase. Table 2 shows that the concentrations were in accordance with the concentrations estimated from the recipe. However, Si was not found in this phase; thus, it was considered to be present as SiO_2 in the nondigestible fraction. The relatively low concentration of calcium in the digestible fraction as compared with the amount of calcium added in the initial preparation also suggested that calcium was present as an oxide in the nondigestible fraction—but only at a trace level compared to SiO_2. Table 3 shows that EDAX also detected an appreciable amount of Cu in the initial sample, in addition to Si, Fe, Al, and Ca. This unexpected presence of Cu was most likely caused by an impurity in one of the reagents used by PNNL in the preparation of the C-103 simulant.

Effect of the Magnetic Field on the Removable Particle Size

Figure 3 shows the VPSDs obtained from the initial sample, as well as from the head, drain, and magnetically retained fractions from the first stage. Although not shown, similar results were obtained with stages 2, 3, and 4. Two peaks were normally observed in all of the samples. The first one, or the small-particle fraction, ranged from 0.5 to 1.5 μm, while the second peak, or the large-particle fraction, ranged from 2 to 14 μm. Compared with the initial sample, the magnetically retained fraction contained a larger proportion of the largest particles and very few small particles. The drain fraction contained a larger proportion of the smallest particle fraction and a larger proportion of the smallest particles from the large particle fraction. Compared with the initial sample, the head fraction contained similar proportions of the large and small particles, but it was devoid of the largest particles. In general, these results showed that the 0.3-T magnetic field was capable of removing only the larger magnetic particles. This result also suggested that most of the species were only weakly magnetic, based on a comparison with the HGMS specifications quoted by the manufacturer.

Figure 4 shows a summary of the mean particle sizes (represented by the bars) and the corresponding dry weight percentages (represented by the symbols and lines) of the large-particle fractions of all the samples from the first four stages and the initial sample. The wt % was based on the g of insoluble solids in each of the samples. Again, the magnetically retained fraction always contained the largest particles and the highest dry weight percentages (>90%). The drain fraction always contained the smallest particles from the large-particle fraction, with dry weight percentages between 83 and 90%. The head fraction was again similar to the initial sample, but it always had a slightly smaller mean particle size and a slightly higher dry weight percentage, on average, among the four stages.

Figures 5 through 8 show SEM pictures from the initial sample, and from the head, drain and magnetically retained fractions from the first stage, respectively. The relative sizes of the particles are in agreement with the VPSDs. For example, the head fraction resembled the initial sample more than either the magnetically retained or drain fractions. Also, the head fraction had a larger range of particle sizes than the

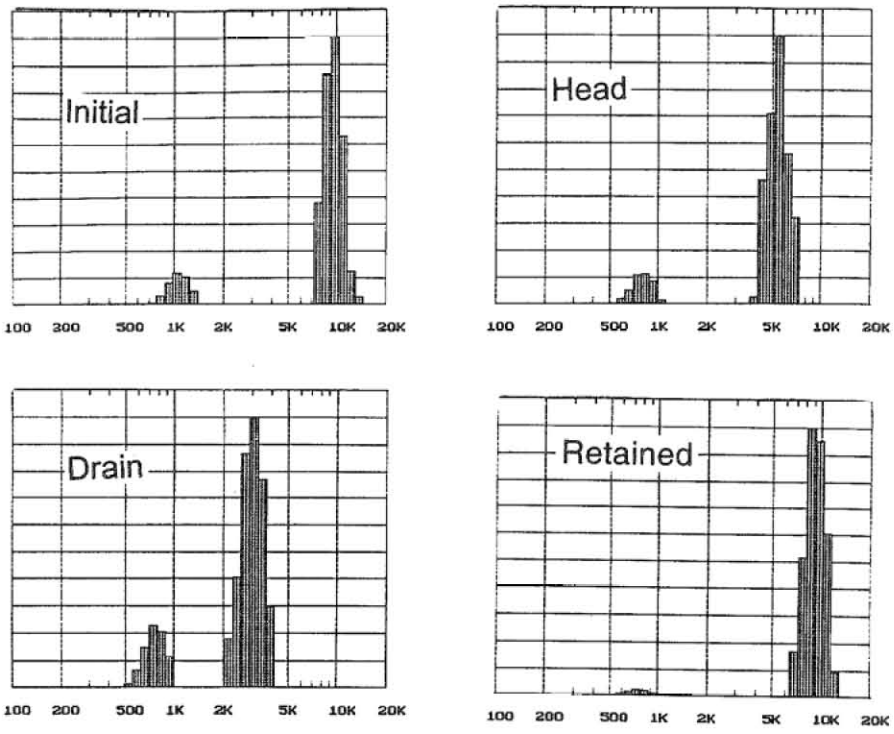

FIGURE 3. Volumetric particle size distributions of the initial sample, and the head, drain, and magnetically retained fractions from the first stage. The particle size unit is in nanometers (nm).

magnetically retained and drain fractions, both of which contained more distinct and larger particles.

Effect of the Magnetic Field on Removal and Segregation of Iron

Table 3 shows the relative weight percentages of Fe, Si, Ca, Al, and Cu in the initial sample, and in the head, drain and magnetically retained fractions obtained by EDAX. The last three rows also show the weight ratios of Fe, Si, and Ca with respect to Al. An important effect of the magnetic field (0.3 T) on the adsorption of Fe was

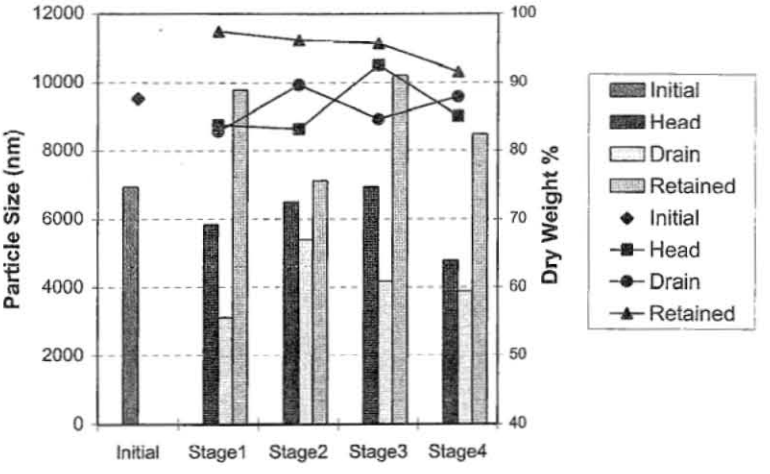

FIGURE 4. Average values (bars) of the mean particle sizes and dry weight percentages (lines and dots) of the large-particle fraction in the initial sample, and in the head, drain, and magnetically retained fractions from the first four stages.

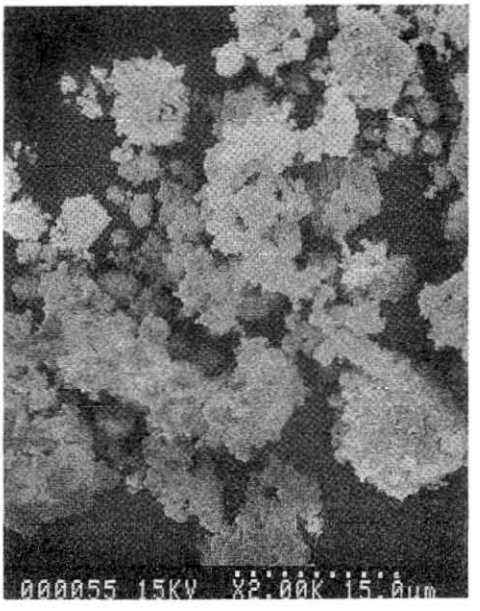

FIGURE 5. SEM micrograph of the initial sample.

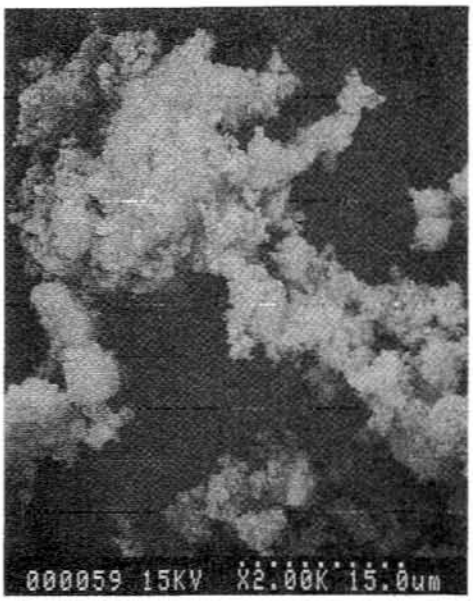

FIGURE 6. SEM micrograph of the head fraction from the first stage.

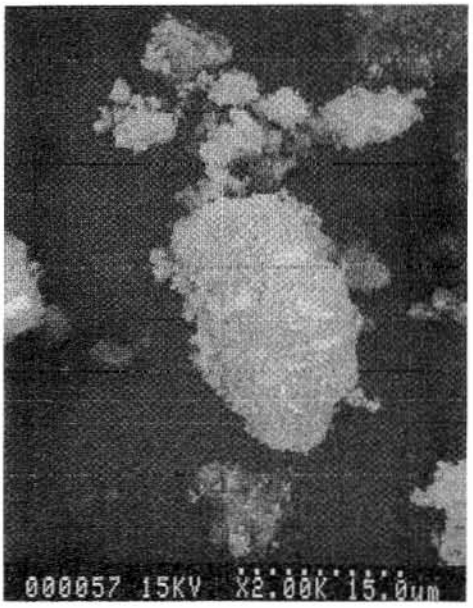

FIGURE 7. SEM micrograph of the drain fraction from the first stage.

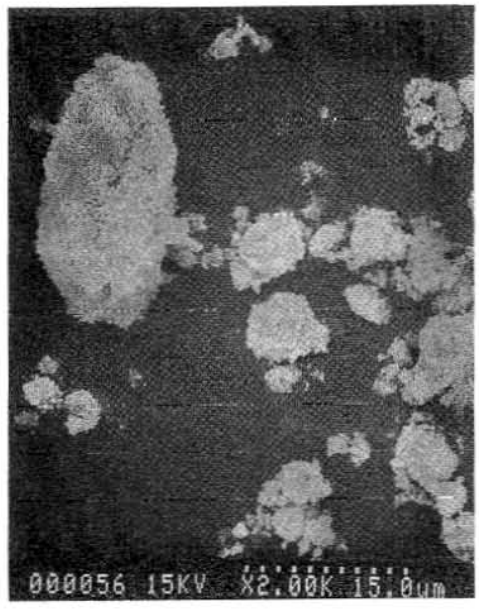

FIGURE 8. SEM micrograph of the magnetically retained fraction from the first stage.

observed. The relative weight percentage of Fe in the magnetically retained fraction was about twice that in the other stages; and the relative weight percentages of the least paramagnetic elements and the diamagnetic elements were less than those in the other stages. However, segregation among the other species (i.e., Si, Al, and Ca) was not significant in all of the samples. This result was expected, since Fe is very paramagnetic as opposed to the other three elements, which have relatively weak and similar diamagnetic properties. Similar results were obtained with the elemental analyses obtained with the flame AA.

Figure 9 shows the dry weight percentages of (a) Fe, (b) indigestible solids (mainly SiO_2), and (c) Al obtained with the flame AA. Figure 9a also shows the weight of sludge removed by the HGMS unit in each stage (circles with lines). As with EDAX, the Fe content was much larger in the magnetically retained fraction. Also, the Fe content in the magnetically retained fraction remained relatively constant throughout the

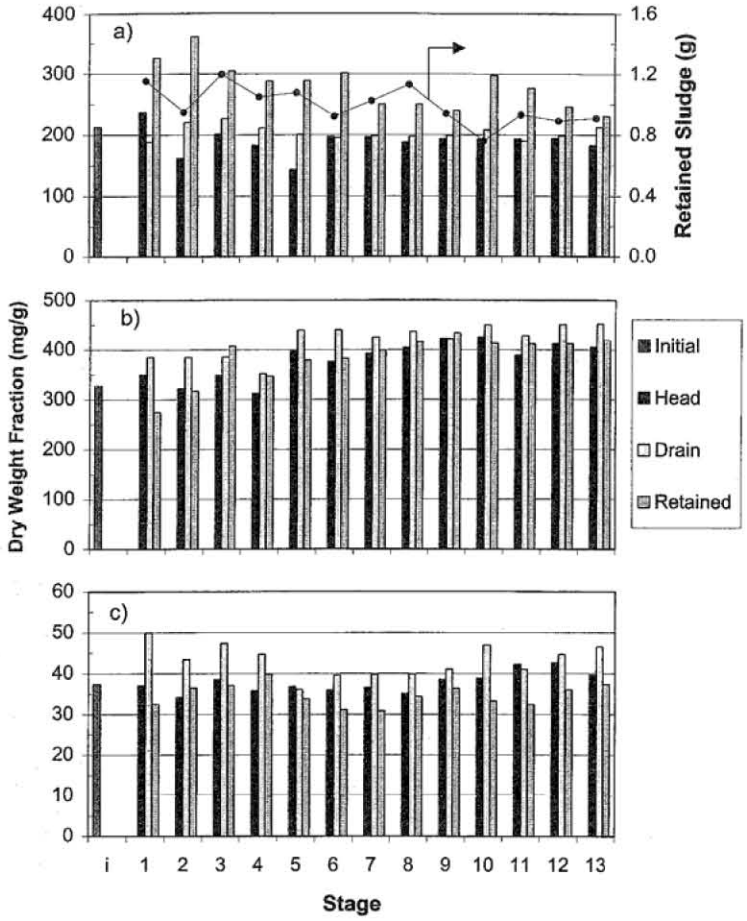

FIGURE 9. (a) Dry-weight percentages of Fe and the amount of sludge removed by the HGMS system, (b) dry-weight percentages of the nondigestible fraction, and (c) dry-weight percentages of Al in the initial, and in the head, drain, and magnetically retained fractions for each of the 13 stages.

13 stages of processing. Clearly, the HGMS unit became saturated during each of the 13 stages, indicating that the working capacity of this bench-scale unit was low relative to the removable Fe in this high-solids-content (99.4 g/L) C-103 sludge simulant. Nevertheless, between 1 and 2% of the total Fe in the sludge was removed during each stage; over 18.5 % was removed in the 13 stages. More stages could have been carried out, but not without diluting the head volume, since the head volume became too small to process through the HGMS unit after the thirteenth stage. In fact, experiments carried out with a highly diluted sludge (40) (insoluble solids content of approximately 10 g/L) showed that this HGMS system is capable of removing more than 99% of the insoluble solids, in agreement with manufacturer's specifications and the trends presented in Figure 9.

Figure 9 also shows that the fractionation between the different species was not great, indicating that the fractionation was essentially based on differences in size of the particles, which undoubtedly had a spectrum of volumetric magnetic susceptibilities. This result suggested that the oxides such as silica, gibbsite, and boehmite were most likely acting as nucleation or coordination agents for the precipitated Fe (i.e., Fe adsorbents), since significant amounts of diamagnetic oxides were present in the magnetically retained fraction. It was also interesting that the drain contained relatively higher concentrations of Al, which can be deleterious to the vitrification process; but the drain solutions were very dilute, and the effect was not pronounced enough to have an effective separation of Al.

CONCLUSIONS

The results obtained in this work showed that HGMS was capable of removing a considerable amount of Fe from C-103 Hanford tank waste simulant with a magnetic field of only 0.3 T. For example, in 13 stages, the bench-scale HGMS unit removed almost 20% of the total Fe in 1-L of sludge with fairly constant loadings in every stage. This latter result also suggested that the unit capacity was low relative to the total removable Fe and that further separation could be carried out. However, along with the higher concentrations of Fe in the magnetically retained fraction, diamagnetic oxides like silica, gibbsite, or boehmite were present in considerable amounts. These oxides are

well known for their adsorptive properties, and their presence in the magnetically retained fraction suggested that they were working as nucleation or coordination agents for the precipitated Fe and thus aiding in the formation of relatively large particles with a wide spectrum of volumetric magnetic susceptibilities. These results also showed that the fractionation was based essentially more on size differences between the particles, as the largest particles were found in the magnetically retained fraction. For example, the HGMS unit was very effective at removing only particles larger than 5 μm, which according to the specifications of the HGMS unit, indicated that the particles were probably composed of Fe in a weakly magnetic state. Also, for sludges with high insoluble solids content (99.4 g/L) and relatively small fields (0.3 T), this HGMS system cannot be used to further concentrate the sludge due to its relatively small loading capacity per column volume (about 4 to 5 g/L). Nevertheless, HGMS seems plausible as a pretreatment step to OGMS to prevent OGMS from clogging in the treatment of HLW.

ACKNOWLEDGEMENTS

The authors gratefully acknowledge financial support from the National Science Foundation under Grant CTS-9520897, from the Argonne National Laboratory under Contract No. 970552401, and from Laidlaw Environmental Services, Inc., in the form of a Graduate Fellowship to A.D.E.

REFERENCES

1. J. H. P. Watson in *Solid-Liquid Separation: High Gradient Magnetic Separation,* 3rd Edition, L. Svarovsky, Ed., Butterworth-Heinemann, Oxford, 1990.
2. J. Iannicelli, IEEE Trans. Magn. *12,* 436 (1976).
3. R. R. Oder, IEEE Trans. Magn. *12,* 428 (1976).
4. J. Svodoba, M. Lazer, and W. A. M. Te Riele, IEEE Trans. Magn. *23,* 283 (1987).
5. F. J. Friedlaender, R. Gerber, H-P. Henkel, and R. R. Birss, IEEE Trans. Magn. *17,* 2804 (1981).
6. F. J. Friedlaender, R. Gerber, W. Kurz, and R. R. Birss, IEEE Trans. Magn. *17,* 2801 (1981).

7. M. Troy, Study of Magnetic Filtration Applications to the Primary and Secondary Systems of PWR Plants, Report NP-514, TPS-76-665, U.S. EPRI, 1978.
8. D. M. Allen, Treatment of Combined Sewer Overflows by High Gradient Separation, Report 600/2-78-209, U.S. EPA, 1976.
9. D. L. Cummings, D. A. Himmelblau, and J. A. Oberteuffer, AIChE J. *22*, 569 (1976).
10. F. E. Luborsky and B. J. Drummond, IEEE Trans. Magn. *11*, 1697 (1975).
11. R. Mitchell, G. Bitton, and J. A. Oberteuffer, Sep. Pur. Methods *4*, 267 (1975).
12. J. A. Oberteuffer, IEEE Trans. Magn. *10*, 223 (1974).
13. J. H. P. Watson, J. Appl. Phys. *44*, 9, 4209 (1973).
14. S. C. Trindade and H. H. Kolm, IEEE Trans. Magn. *9*, 310 (1973).
15. J. A. Oberteuffer, IEEE Trans. Magn. *9*, 303 (1973).
16. L. A. Worl, D. D. Hill, D. D. Padilla, and F. C. Prenger, High Gradient Magnetic Separation for Nuclear Material Collection, U.S. DOE Report LANL LA-UR-97-1508, 1997.
17. L. R. Avens, Use of High Gradient Magnetic Separation for Actinide Applications, U.S. DOE Report LANL LA-UR-96-2064, 1996.
18. A. R. Schake, L. R. Avens, D. D. Hill, D. D. Padilla, F. C. Prenger, D. A. Romero, T. L. Tolt, and L. A. Worl, Magnetic Separation for Environmental Remediation, U.S. DOE Report LANL LA-UR-94-3373, 1994.
19. F. C. Prenger, W. F. Stewart, D. D. Hill, L. R. Avens, A. R. Schake, K. J. de Aguero, D. D. Padilla, L. A. Worl, and T. L. Tolt, High Gradient Magnetic Separation Applied to Environmental Remediation, U.S. DOE Report LANL LA-UR-93-2516, 1993.
20. L. R. Avens, L. A. Worl, K. J. de Aguero, F. C. Prenger, W. F. Stewart, D. D. Hill, and T. L. Tolt, "Environmental Remediation using Magnetic Separation, "presented at the AIChE Annual Meeting", Miami Beach, Florida, November 1992.
21. C. Tsouris and T. C. Scott, J. Colloid Interface Sci. *171*, 319 (1995).
22. C. Tsouris, S. Yiacoumi, and T. C. Scott, Chem. Eng. Commun.*137*, 147 (1995).
23. C. Tsouris, T. C. Scott, and M. T. Harris, Sep. Sci. Technol. *30*, 1407 (1995).
24. S. Yiacoumi, D. A. Rountree, and C. Tsouris, J. Colloid Interface Sci. *184*, 477 (1996).

25. C. Tsouris and S. Yiacoumi, Sep. Sci. Technol. *32*, 599 (1997).
26. C. Latour and H. Kolm, IEEE Trans. Magn. *11*, 1570 (1975).
27. C. Latour, IEEE Trans. Magn. *9*, 314 (1973).
28. B. B. Emory, IEEE Trans. Magn. *17*, 3296 (1981).
29. R. R. Dauer and E. H. Dunlop, Biotechnol. Bioeng. *37*, 1021 (1991).
30. S. Miltenyi, W. Muller, W. Weichel, and A. Radbruch, Cytometry *11*, 231 (1990).
31. G. Bitton, G. F. Gifford, and O. C. Pancorbo, Removal of Viruses from Water by Magnetic Filtration, Report PB-261494, U.S. NTIS, 1976.
32. M. Ublen, E. Hornes, and O. Olsvik, Advances in Biomagnetic Separation, Eaton Publishing Co., 1994.
33. J. A. Ritter, J. R. Zamecnik, N. D. Hutson, M. E. Smith, and J. T. Carter, Water Sci. Technol. *25*, 269 (1992).
34. C. M. Jantzen, J. Am. Ceram. Soc. *75*, 2433 (1992).
35. A. S. Holman et al., Initial Investigation of Open-Gradient Magnetic Separation, Oak Ridge National Laboratory Report ORNL-5754, April 1982.
36. K. J. de Aguero, U. F. Gallegos, and L. R. Avens, Magnetic Separation of Bomb-Reduction Sand, Graphite, and Sand, Slag, and Crucible Residues, Los Alamos National Laboratory Report LA-12011-MS, July 1991.
37. R. D. Doctor, Process for Magnetic Beneficiating Petroleum Cracking Catalyst, U.S. Patent 5,250,482 (1993).
38. R. D. Doctor, C. B. Panchal, and C. E. Swietlik, in Recent Advances in Separation Techniques-III, N.N. Li, Ed., American Institute of Chemical Engineers Symp. Series *82* (250), 154 (1986).
39. L. Nuñez, R. Doctor. and A. Visser, "Superconducting Open-Gradient Magnetic Separation for the Pretreatment of Radioactive or Mixed Waste Vitrification Feeds," presented at the Tenth Symposium on Separation Science and Technology for Energy Applications, Gatlinburg, Tennessee, 1997.
40. A. D. Ebner and J. A. Ritter, unpublished results (1998).